RIGOROUS GENERATION OF DIGITAL ORTHOPHOTOS FROM EROS A HIGH RESOLUTION SATELLITE IMAGES

Liang-Chien CHEN and Tee-Ann TEO

Center for Space and Remote Sensing Research, National Central University, 320 Chung-Li, TAIWAN
Tel: +886-3-4227151ext7622 Fax: +886-3-4255535 Email: lcchen@csrsr.ncu.edu.tw

Commission IV, WG IV/7

ABSTRACT:

As the resolution of satellite images is improving, the applications of satellite images become widespread. Orthorectification is an indispensable step in the processing for satellite images. EROS A is a high resolution imaging satellite. Its linear array pushbroom imager is with 1.8meter resolution on ground. The satellite is sun-synchronous and sampling with asynchronous mode. The main purpose of this investigation is to build up a procedure to perform orthorectification for EROS A satellite images. The major works of the proposed scheme are:(1) to set up the transformation models between on-board data and respective coordinate systems, (2) to perform correction for on-board parameters with polynomial functions, (3) to adjust satellite's orbit using a small number of ground control points, (4) to fine tune the orbit using the Least Squares Filtering technique and, (5) to generate orthoimage by using indirect method. The experiment includes validation for positioning accuracy using ground check points.

1. INTRODUCTION

The generation of orthoimages from remote sensing images is an important task for various remote sensing applications. Nowadays, most of the high resolution satellites are using linear pushbroom arrays, such as IKONOS, Quickbird, EROS and others. From the photogrammetric point of view, base on the collinearity condition equations; bundle adjustment may be applied to model the satellite orientation (Guaan and Dowman 1988, Chen and Lee 1993). This approach needs a large number of ground control points (GCPs). Chen and Chang (1998) used on-board data and a small number of GCPs to build up a geometric correction model for SPOT satellite images. Similarly, we will propose to use the on-board orbital parameters and GCPs to calibrate the satellite orbit. After orbit modelling, we will develop an indirect method to do the image orthorectification.

2. CHARACTERISTICS OF EROS A SATELLITE

EROS A was launched by ImageSat International (ISI) on the 5th of December, 2000. It is expected to have at least four years of lifetime. Its orbit altitude is 480km with 97.3 degrees orbit inclination, which make the satellite sun-synchronous. Using its body rotation function, the satellite is able to turn up to 45 degrees in any direction. Its linear array pushbroom imager is with 1.8meter resolution on ground and 1.5degree of field of view. Table 1 shows the characteristics of EROS A satellites.

EROS A satellite takes images with asynchronous mode. It allows the satellite to move in a faster ground speed than its rate of imaging. The satellite actually bends backwards to take its images in an almost constant, predetermined angular speed, enabling its detectors to dwell longer time over each area. In this way, it will be able to get lighter, and improve contrast and

conditions for optimal imaging. Fig 1(a) illustrates the synchronous mode vs. asynchronous one. Referring to fig. 1(b),

the satellite orbit is longer than the sampling area. In the best condition, the ratio of satellite orbit to sampling area is about 1 to 5

Table I. The characteristics of EROS A satellites

| ITEM	EROS A Specification
Orbit Altitude	480km
Orbit Inclination	97.3 Deg
Orbit Pass rate	15.3 orbits/day
Body Rotation	Yes
Mode of Operation	Push Broom Scanning
Scanning Mode	Asynchronous (up to 750 lines/sec)
Stereo pairs	In Track, Cross Track
Sensor Type	CCD
Swath Width	12.5km
Ground Sampling Distance	1.8m (PAN)
Focal Length	3.4 m
Slant Angles	45 Deg
Field of View	1.5 Deg
Pixels-in-line	7800
Spectral Band	Panchromatic:0.5 to 0.9 µm
Sampling Depth Transmitted	11 Bits

(a)

(b)
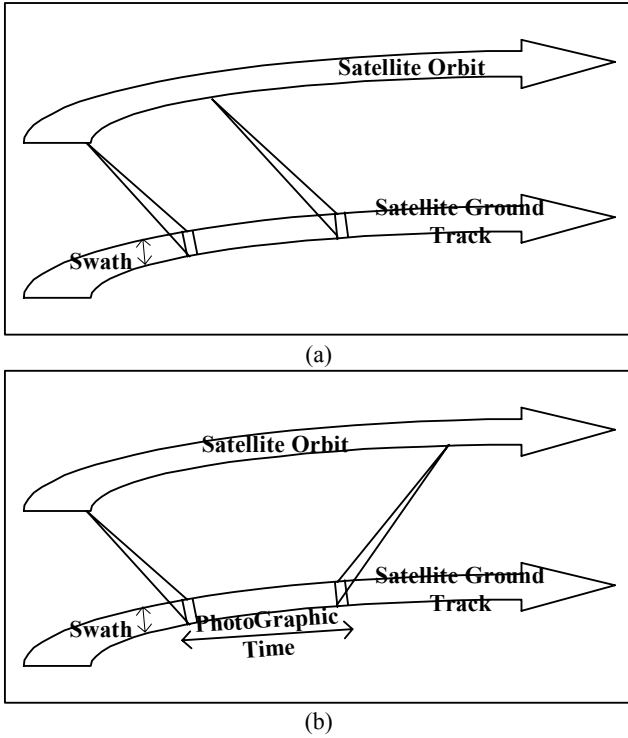
Figure 1. Illustration for scanning modes (a) Synchronous (b) Asynchronous

3. METHODOLOGY

The proposed method comprises two major parts. The first part is to build up the satellite orientation by using the ground control points. The second one is to use the orbit parameters to perform the orthorectification.

3.1 Orientation Modeling

The major step in validating the positioning accuracy for an image is to model the orbit parameters and the attitude data. Once those exterior orientation parameters are modeled, the corresponding ground coordinates for an image pixel can be calculated. Due to the extremely high correlation between two groups of orbital parameters and attitude data, we only correct the orbital parameters. That means, we will use the attitude information in the on-board ephemeris data as known values.

Three steps are included in this investigation. The first step is to initialize the orientation parameters using on-board ephemeris data. We then fit the orbital parameters with second-degree polynomials using GCPs.

Once the trend functions of the orbital parameters are determined, the fine-tuning of an orbit is performed by using Least Squares Filtering (also called "Least Squares Collocation") technique.

3.1.1 Initialization Of Orientation Parameters: The on-board ephemeris data and GCPs are in different coordinate systems. Before the orbit adjustment, it is essential to build up the coordinate transformation, so that the orbit adjustment will be performed in WGS84 as unified coordinate system. Those coordinate systems include inertial frame, WGS84, GRS67, Geodetic Coordinate System, TWD67, Orbital Reference Frame and EROS A Body Frame. In which, GRS67 used the Kaula ellipsoid (a=6378160m, f=1/298.247). The Geodetic Coordinate System is in longitude and latitude. Based on the datum of GRS67, the TWD67 system is a Transverse Mercator Projection using λ =121E as the central meridian. There will be three steps between TWD67 and WGS84 transformation. First, we project TWD67 into the Geodetic Coordinate System, then the Geodetic Coordinate System is projected into GRS67. Finally, the GRS67 system is transformed into WGS84. The camera model was provided by ISI International.

3.1.2 Preliminary Orbit Fitting: Because the on-board data includes errors to a certain degree, GCPs are needed to adjust the orbit parameters. Referring to fig. 2, the observation vector (Ua) provided by the satellite will not pass through the corresponding GCP due to errors the on-board data. Thus, correction of the orbit data from (x_0, y_0, z_0) to (x, y, z) may be performed under the conditions

$$X_i = x(t_i) + S_i u_{x_i} \qquad (1a)$$

$$Y_i = y(t_i) + S_i u_{Y_i} \qquad (1b)$$

$$Z_i = z(t_i) + S_i u_{Z_i} \qquad (1c)$$

$$x(t_i) = x_0 + a_0 + a_1 \cdot t_i + a_2 \cdot t_i^2 \qquad (2a)$$

$$y(t_i) = y_0 + b_0 + b_1 \cdot t_i + b_2 \cdot t_i^2 \qquad (2b)$$

$$z(t_i) = z_0 + c_0 + c_1 \cdot t_i + c_2 \cdot t_i^2 \qquad (2c)$$

where
X_i, Y_i, Z_i are object coordinates of the ith GCP,
u_{xi}, u_{yi}, u_{zi} are components of the observation vector,
$x(t_i)$, $y(t_i)$, $z(t_i)$ are the satellite's coordinates of the ith GCP after correction,
x_0, y_0, z_0 are the satellite's coordinates before correction,
a_i, b_i and c_i (i=0,1,2) are coefficients for orbit corrections,
t represents sampling time, and
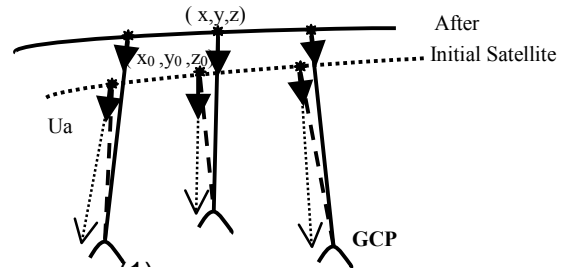S_i is the scale factor.

Figure 2. Preliminary fitting for satellite orbit

3.1.3 Least Squares Filtering: Because the least squares adjustment is a global treatment, it cannot correct for the local errors. Therefore, the least squares filtering (Mikhail and Ackermann, 1982) has to be used to fine tune the orbit. By doing this, we assume that the x, y, z-axis are independent. Thus, we use three one-dimensional functions to adjust the orbit. The model of least squares filtering is shown as

$$\rho_k = \vec{v}_k \; [\; \Sigma_k \;]^{-1} \; \vec{\varepsilon}_k \tag{3}$$

where

k is x,y,z axis

ρ_k is the correction value of the interpolating point ,

$\vec{v}_k$ is the row covariance matrix of the interpolating point with respect to GCPs,

Σ_k is the covariance matrix for GCPs, and

$\vec{\varepsilon}_k$ is the residual vectors for GCPs.

The basic consideration in this investigation is to minimize the number of required GCPs. Thus, using a large amount of GCPs to characterize the covariance matrix is not practical. In this paper, we use a Gaussian function (shown as fig. 3) with some empirical values as the covariance function. The Gaussian function is shown as

$$Covariance = \begin{cases} c\,e^{-(2.146\frac{d}{d_{max}})^2} & , \quad if \quad d \neq 0 \\ \mu_k & , \quad if \quad d = 0 \end{cases} \tag{4}$$

$$c = (1 - r_n)\,\mu_k$$

where

d is the distance between an intersection points and a GCP,

d_{max} is the distance between an intersection point and the farthest GCP,

μ_k is the variance of GCPs' residual, and

r_n is the filtering ratio, in which we use r_n=0.1 in experiment.

The empirical value 2.146 is selected so that the covariance limit is 1% of $0.01(1- r_n)\mu_k$ when d=dmax (Chen & Chang, 1998).

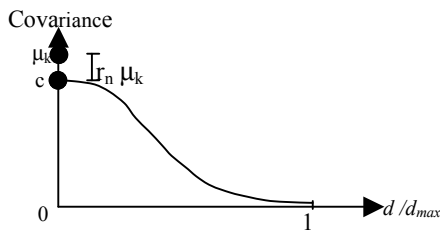Figure 3. Covariance function of least squares filtering

3.2 Orthorectification

There are two ways to do the orthorectification. The first one is the direct method. A technique called Ray-Tracing (O'Neill and Dowman, 1988) was developed to solve the problem by direct method. It projects a 2D image point on to a 3D object model. The second one is indirect method, which projects the 3D object point on to 2D image space. It is known that the indirect method performs better than the direct method in terms of efficiency and quality (Mayr and Heipke 1988,Chen and Lee 1993). We select the indirect method to determine the corresponding image pixels from a ground element.

Once the orientation parameters are determined and a DTM is given, the corresponding image position for a ground point may be determined by the indirect method. Fig. 4 shows the geometry of indirect method. Given a ground point **A**, we can create **a** vector **r(t)** from ground point **A** to image point **a**. The vector **r(t)** vector is located on the principle plane and **n(t)** is the normal vector on the principal plane. The mathematics show that, at time t, **r(t)** is orthogonal to the normal vector **n(t)**. When **r(t)** is perpendicular to **n(t)**, the inner product of **r(t)** and **n(t)** is zero. The function **f(t)** is defined to characterize the coplanarity condition

$$f(t)=r(t) \cdot n(t)=0 \tag{5}$$

We apply Newton-Raphson method to solve the nonlinear equation (5), to determine the sampling time t for ground point **A**. The iteration is expressed in the equation (6),

$$t_{n+1} = t_n - \frac{f(t_n)}{f'(t_n)} = t_n - \frac{f(t_n)}{[f(t_n+\Delta t) - f(t_n - 2\Delta t)]/2\Delta t} \tag{6}$$

when n=0,1,2….. until $|t_{n+1}-t_n|<10^{-5}$ sec is satisfied.
For an image point sampled at time t, we can decide a principal plane, the along track image coordinate can be calculate by

Line=(t-t0)/(integration time) (7)
where t0 is sampling time for the first scan line. Integration time is the sampling interval.
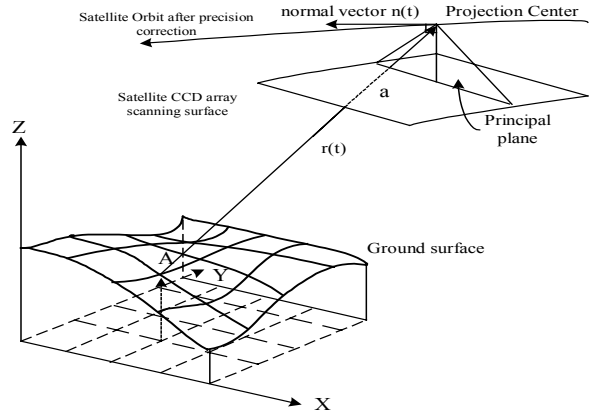

FIGURE 4. Illustration of indirect method

The across track image coordinate may be determined, as shown in fig. 5. In the figure, V_f is the pointing vector of first CCD in line, and V_l is the pointing vector of last CCD in line. The across track coordinate for the pixel is

Sample=(S/FOV)*7043 (8)

where

S is the angle between V_f and **r(t)**.

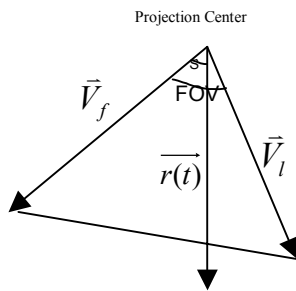FOV is field of View angle, and

7043 is number pixel in a line.

Figure 5. Illustration for determining across-track image coordinate

4. EXPERIMENTS

The experiments include two parts of validation. The first one is to check for the determined orientation parameters. The second one is to examine the accuracy for the generated orthoimage

4.1. Test Data

The test area is in KaoHsiung, which is located in the southern part of Taiwan as shown in fig.6. Scene ID is TAW1-e1019903, which were sampled on Apr. 15, 2001. The asynchronous ratio of the satellite orbits to sampling area is 1:13. The GCPs and check points (CHKPs) were measured from 1:1000 scale topographic maps. The position accuracy is better than 50 centimeters. The distributions of those points are shown in fig. 6. In the figure, triangles represent the GCPs while boxes are the CHKPs. The total number of GCPs and CHKPs are 53. Other related information is shown in Table II.
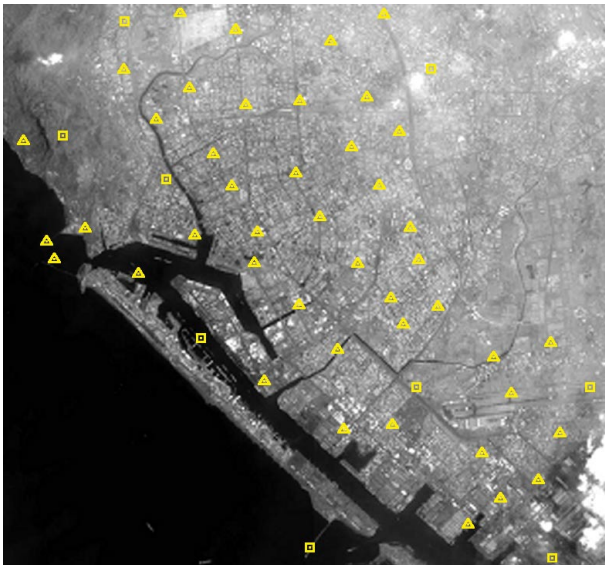
©ImageSat International 2001.
Figure 6. The test image.

Table II. Related information of test images

ITEM	Parameters
Scene ID	TAW1-e1019903
Date	2001/04/15
Integration Time	3.7msec
Ground Sampling Distance	1.90m
Test Area	13.38km * 12.48km
Image size	7043* 6572 pixel
Place	KaoHsiung, Taiwan
Pointing Angle	11.60 Deg
Orbit Arc	170KM(about 1:13)

The DTM used in the orthorectification was acquired from the Topographic Data Base of Taiwan. The pixel spacing of DTM is resample from 40m to 2m. Fig. 7 illustrates the terrain variation. The elevation ranges from 0m to 340m.
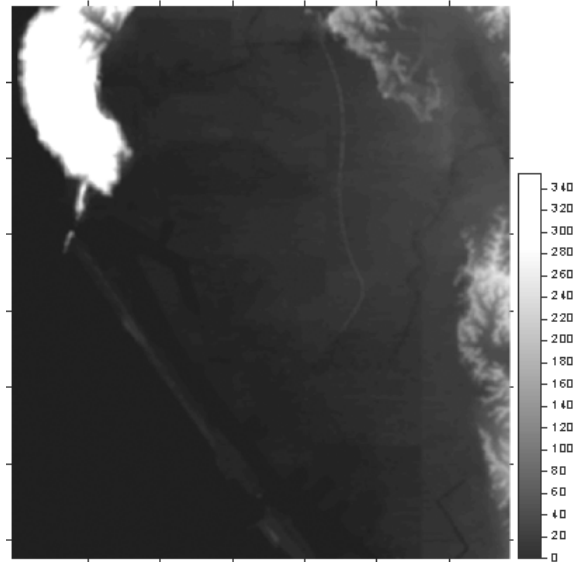

Figure 7. The DTM used in orthorectification

4.2. Accuracy VS. Number of GCPs

The Ray-Tracing method is applied to evaluate the orbit accuracy. Given the satellite orientation and image point, we calculate the intersection point of DTM and ray direction. Fig.8 indicates the RMSEs when different numbers of GCPs were employed in the test data. Table III lists the figures to indicate the trend in detail. It is obvious that the RMSEs i.e., (3.53m, 4.70m) tend to be stable when 9 or more control points were employed. Notice that the coordinate system is in TWD67 with Transverse Mercator projection.
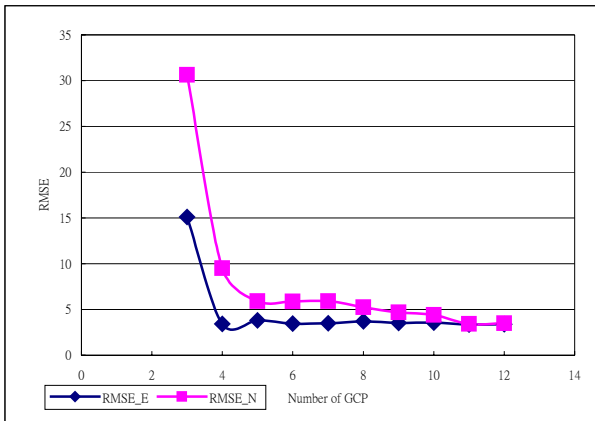
Figure 8. RMSEs for the different number of GCPs

Table III. RMSEs for different number of GCPs

| No. of GCPs	RMSE E (m)	RMSE N (m)
1	22.17	37.85
2	10.96	32.31
3	15.11	30.64
4	3.41	9.51
5	3.80	5.90
6	3.45	5.86
7	3.48	5.90
8	3.70	5.24
9	3.53	4.70
10	3.55	4.42
11	3.34	3.43
12	3.38	3.50

4.3. Accuracy Analysis Of Orbit Modeling

We further evaluate the error behaviours in the two different phases. Fig.9(a) depicts the error behaviour after preliminary orbit fitting in TWD67 coordinate system. We could see that the system errors are obvious. Fig.9(b) illustrates the results after precision correction, i.e., least squares filtering. The coordinate system is also in TWD67. After using least squares filtering to fine tune the orbit, the major system errors have been compensated.

We provide Table III for the summary of accuracy. Table IV illustrates the accuracy performance of GCPs and CHKPs, when 9 GCPs were employed. After preliminary orbit fitting, the RMSE of CHKPs is about 6meter and 24meter in two directions. After least squares filtering, the RMSE of CHKPs are reducing to 3.3meter and 4.3meter respectively.
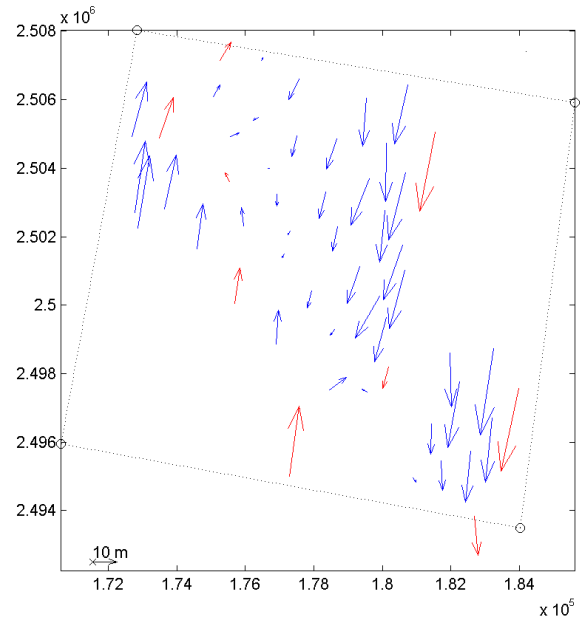
(a)
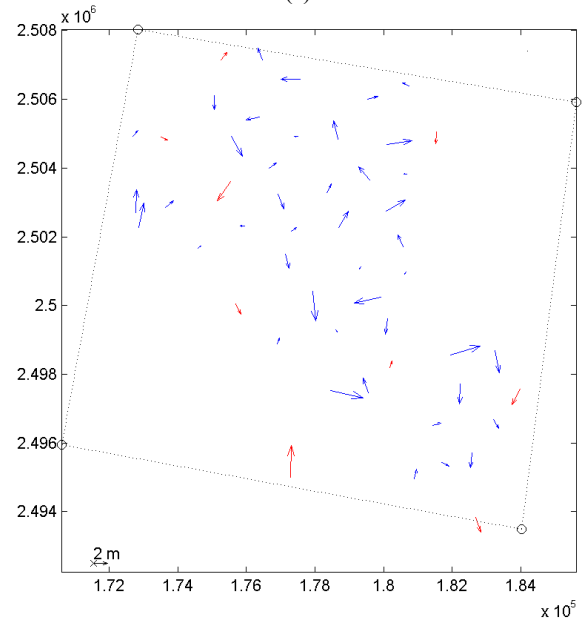
(b)

Figure 9.Error vectors of orbit modeling (a)Error vectors of the preliminary orbit fitting (b) Error vectors after least squares filtering

Table IV. Root-Mean-Square Error of orbit modeling

	RMSE E (meter)	RMSE N (meter)
Preliminary orbit fitting		
GCPs (9)	6.17	30.47
CHKPs (44)	5.63	23.57
Least Squares Filtering		
GCPs (9)	1.47	2.72
CHKPs (44)	3.34	4.37

4.4. Accuracy Evaluation Of Orthorectification

The generated orthoimage is shown in fig. 10. In order to evaluate the quality of orthoimage, we check it manually. Fig. 11 illustrates that the RMSE of ground check point is slightly

better than 2 pixels. It is observed that the error vectors are similar to the result after least square filtering. Table V shown the Root-Mean-Square Error of orthoretification. The RMSEs of CHKPs are 3.1meter and 3.7meter in E and N directions respectively.
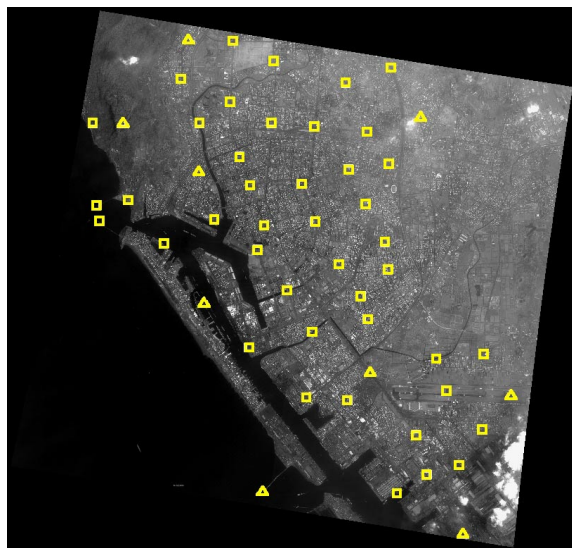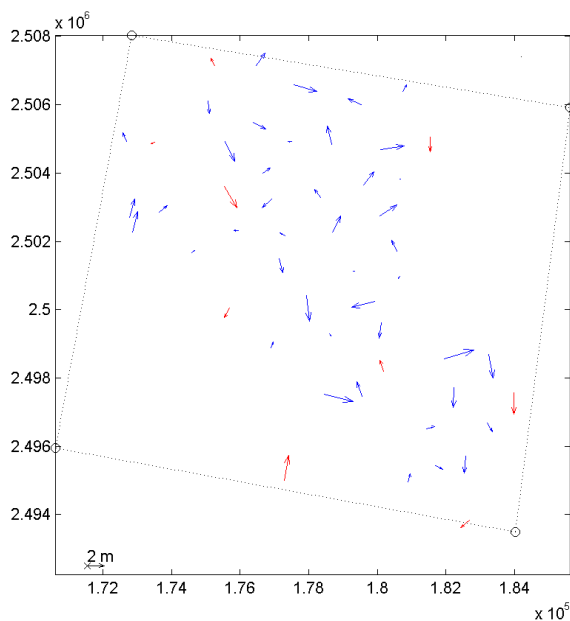

Figure 10. Generated orthophoto

Figure 11.Error vectors for the generated orthophoto

Table V. Root-Mean-Square Error of orthoretification

	Orthorectification	
	RMSE E (meter)	RMSE N (meter)
GCPs (9)	1.80	3.10
CHKPs (44)	3.13	3.74

5. CONCLUSIONS

We have proposed a procedure to perform geometric correction for EROS A satellite images using a small number of GCPs. The corrections for orbital data are modeled as functions of time. The GCPs are applied to correct the on-board data to maintain the geometrical relationship between image space and object space. After that, we use least squares prediction to fine-tune the orbit. Finally, we use indirect method to generate the orthophotos. Experimental results indicate that the proposed scheme may reach an accuracy of better than two pixels in the image scale for an image sampled with an asynchronous ratio of 13. Because of the measurement error, the results of orthorectification and least squares filtering are slightly different. The DTM used in the orthorectification was resampled from the one with 40m resolution. Due to its error, the precision of the proposed method could be underestimated.

6. REFERNENCES

Chen, L.C., and Chang, L. Y., 1998, "Three Dimensional Positioning Using SPOT Stereostrips with Sparse Control", Journal of Surveying, ASCE 124(2): pp.63-72.

Chen, L.C., and Lee, L.-H. 1993, "Rigorous Generation of Digital Orthophoto from SPOT Images." Photogrammetric Engineering and Remote Sensing, 59(5), 655-661.

Gugan, D.J., and Dowman, I. J. 1988, "Accuracy and completeness of topographic mapping from SPOT imagery." Photogrammetric Record, 12(72), 787-796.

Mikhail E.M and F. Ackermann, 1982, Observation and Least Squares, University Press of America, New York, pp.401.

Mayer, W. and C. Heipke, 1988, "A Contribution to Digital Orthophoto Generation", International Archives of Photogrammetry and Remote Sensing, 27(B11):IV430-IV439.

O'Neill, M.A., and Dowman, I. J., 1988, "The Generation of Epipolar Synthetic Stereo Mates for SPOT Images Using a DEM", International Archives of Photogrammetry and Remote Sensing, Kyoto, Japan, 27(B3): pp.587-598.